

# Investigations on pure and Ag doped lithium lanthanum titanate (LLTO) nanocrystalline ceramic electrolytes for rechargeable lithium-ion batteries

K.P. Abhilash<sup>a</sup>, P.Christopher Selvin<sup>a,\*</sup>, B. Nalini<sup>b</sup>, P. Nithyadharseni<sup>c</sup>, B.C. Pillai<sup>c</sup>

<sup>a</sup>N.G.M. College, Pollachi, Coimbatore 642001, India

<sup>b</sup>Department of Physics, Avinashilingam University for Women, Coimbatore 641 017, India

<sup>c</sup>Centre for Research in Nanotechnology, Karunya University, Coimbatore 641114, India

Received 4 June 2012; received in revised form 4 July 2012; accepted 4 July 2012

Available online 3 August 2012

## Abstract

The nano-crystalline  $\text{Li}_{0.5}\text{La}_{0.5}\text{TiO}_3$  (LLTO) was prepared as an electrolyte material for lithium-ion batteries. The effect of  $\text{Ag}^+$  ion doping in three different concentrations were investigated:  $\text{Ag}_{0.1}\text{Li}_{0.4}\text{La}_{0.5}\text{TiO}_3$ ,  $\text{Ag}_{0.3}\text{Li}_{0.2}\text{La}_{0.5}\text{TiO}_3$ , and  $\text{Ag}_{0.5}\text{La}_{0.5}\text{TiO}_3$  along with  $\text{Li}_{0.5}\text{La}_{0.5}\text{TiO}_3$ . The prepared pure and  $\text{Ag}^+$  doped LLTO were subjected for structural, morphological, electrical and optical characterizations. The cubic superlattice structure of LLTO nano-powder was altered due to the  $\text{Ag}^+$  substitution tending towards a tetragonal phase. Increasing  $\text{Ag}^+$  substitution a complete tetragonal phase occurs in  $\text{Ag}_{0.5}\text{La}_{0.5}\text{TiO}_3$ . The average particle size of the prepared ceramic electrolyte ranged between 80 nm and 120 nm. The photoluminescence study reveals that the LLTO and Ag doped LLTO gives a blue emission peak. The size effect on grain and grain boundary resistance was observed and reported. With  $\text{Ag}^+$  substitution, the conductivity got decreased due to the impedance caused by  $\text{Ag}^+$  ions in the conducting path of  $\text{Li}^+$  ion. Among all the samples,  $\text{Ag}_{0.5}\text{La}_{0.5}\text{TiO}_3$  shows maximum conductivity of the order of  $10^{-3} \text{ S cm}^{-1}$ .

© 2012 Elsevier Ltd and Techna Group S.r.l. All rights reserved.

**Keywords:** B. Nanocomposites; C. Ionic conductivity; D. Perovskites; E. Batteries

## 1. Introduction

In this modern times of energy crisis, development of more efficient and viable sources of energy and their storage devices such as lithium ion batteries have proven its own importance. The thrust of scientific research is directed for technological incentives to the development of more efficient ways of converting and storing a large amount of energy in a small package, light in weight and safe to use. The development of all solid state lithium ion batteries has received considerable attention because of their application potential to the new generation energy sources using less stringent assembling condition which enables the mass production. However the main impediment is finding a new sound solid electrolyte that has reasonably high lithium ionic conductivity and good stability. To date, the fastest lithium ion conducting

electrolytes are the Perovskite type ( $\text{ABO}_3$ ) lithium lanthanum titanate  $\text{Li}_{3x}\text{La}_{2/3-x}\text{TiO}_3$  (LLTO) and their derivatives [1–3]. In this structure there are a substantial number of “A” site vacancies created by the disordered arrangement of Li and La ions, which facilitates the lithium ion transport [4]. The LLTO has a room temperature bulk conductivity of about  $10^{-3} \text{ Scm}^{-1}$  [5]. However its grain boundary conductivity is quite low and of the order of  $10^{-5} \text{ Scm}^{-1}$  [6]. To migrate from one A site to the next available site  $\text{Li}^+$  ions have to pass through a bottleneck made of four surrounding oxygen atoms [7]. To increase the ionic conductivity, many attempts have been made and discussed in the literature. This has been performed by the substitution of ions on either the A site or the B site of the Perovskite structure [8,9].

In 2002, Nalini et.al. [10] had reported the  $\text{Eu}^{2+}$  substitution on the ‘B’ sites of LLTO perovskite and the conductivity is found to be improved in the doped samples. Small amount of aluminum replacing the titanium have

\*Corresponding author. Tel.: +91 9486243082; fax: +91 4259 234869.

E-mail address: pcsphyngmc@rediffmail.com (P. Christopher Selvin).

been shown to lead to high conductivity. The replacement of some oxygen with fluorine does not significantly affect the conductivity [11]. Another study shows that the addition of silica to  $\text{Li}_{0.5}\text{La}_{0.5}\text{TiO}_3$  increases total conductivity [11]. In 2010 Chen et.al. [9] had reported the Raman Spectra and EXAFS studies on Na and Nd substituted LLTO ceramics. Further recent studies have shown that the specific capacity, corresponding to the charge storage in the bulk of the active materials and cyclability which is the retention capacity during successive charge/discharge cycles, depends on the synthetic route employed for its preparation. One of the effective way to improve the cyclability and storage capacity of this material is to reduce the LLTO particle size to a few nanometers [1]. The reports on nanocrystalline LLTO is very scarce in the literature. As Ag is a very good conductor by itself, the present study makes an attempt to substitute monovalent  $\text{Ag}^+$  ions in the LLTO ‘nano’crystalline host.

The aim of the present work is to establish the nano-size effect of the sol–gel prepared, cubic perovskite structured lithium lanthanum titanate with super lattice lines. The studies also include the changes in structure and electrical conductivities of the samples while the  $\text{Ag}^+$  ions substituted in the A sites of the LLTO perovskite cage.

## 2. Experimental details

Generally the synthesis of LLTO is accomplished by conventional solid state reactions. The conventional preparation needs high temperature sintering, which results in serious lithium loss. As an alternative, modified sol–gel method, which can be used to prepare powder (micro and nano-spheres) or thin films by dip coating/spin coating has been reported to prepare LLTO ceramics [2,12–15]. The  $\text{Li}_{0.5}\text{La}_{0.5}\text{TiO}_3$  (Sample A) has been synthesized by sol–gel method. Lithium nitrate (AR-99.5%, Aldrich), lanthanum nitrate hexahydrate (AR-99%, Himedia), tetra butyl titanate (AR-99%, Aldrich) and acetyl acetone (acac) (AR-99%, Himedia) were used as the raw materials.

The  $\text{LiNO}_3$  and  $\text{La}(\text{NO}_3)_3 \cdot 6\text{H}_2\text{O}$  were weighed in terms of the stoichiometric composition of  $\text{Li}_{0.5}\text{La}_{0.5}\text{TiO}_3$  and dissolved in ethylene glycol monomethyl ether and afterwards they were mixed with the mixture solution of tetrabutyl titanate and acetyl acetone. The precursor sol–gel was calcined at  $900^\circ\text{C}$  for 6 h to yield pure LLTO white powder. The calcined powder was dried and pelletized using the pelletizer by applying a uniform pressure of  $33\text{ kN/m}^2$ . As high temperature sintering will result in growth of the crystalline size, in the present attempt the sintering temperature is reduced to  $300^\circ\text{C}$ . The LLTO sample is doped with silver ( $\text{Ag}^+$  ion) in 3 different concentrations. They are indicated as:

- Sample B:  $\text{Ag}_{0.1}\text{Li}_{0.4}\text{La}_{0.5}\text{TiO}_3$ ; [Ag:Li = 1:4]  
 Sample C:  $\text{Ag}_{0.3}\text{Li}_{0.2}\text{La}_{0.5}\text{TiO}_3$ ; [Ag:Li = 3:2]  
 Sample D:  $\text{Ag}_{0.5}\text{La}_{0.5}\text{TiO}_3$ ; [Ag:Li = 5:0] (Without any Li content)

The  $\text{Ag}^+$  doped samples were prepared by using  $\text{AgNO}_3$  along with other raw materials in the stoichiometric ratios mentioned above.

The prepared LLTO and  $\text{Ag}^+$  doped LLTO powders were structurally characterized by powder XRD technique (XRD-SHIMADZU-6000) diffractometer using  $\text{Cu K}\alpha$  radiation source. The morphological characterizations of the samples were carried out using SEM (JEOL-JSM 6390) and EDX (OXFORD INCA ENERGY Mn 137 keV). The samples were optically characterized by using Spectro Fluorimeter (HORIBA-FLOUROLOG®-3). The electrical characterizations of the samples were carried out by Complex Impedance Spectrometer (SOLATRON 1260) using silver paste as the contact electrode.

## 3. Result and discussion

Fig. 1 shows the powder XRD pattern of pure and  $\text{Ag}^+$  doped LLTO samples. The  $\text{Li}_{0.5}\text{La}_{0.5}\text{TiO}_3$  (LLTO) shows a cubic perovskite structure with characteristic broadening of the peaks associated with the size reduction in the XRD pattern. The XRD peaks were assigned to cubic perovskite structure and found that a few of the peaks were emerged due to superlattice structure which is indicated by asterisk (\*) in Fig. 1. The result falls in line with the work done by Nalini et al. [10] on LLTO. Here as the cubic structure is highly ordered, the diffraction peaks would correspond to the cubic sites with an interplanar distance “a” and also the

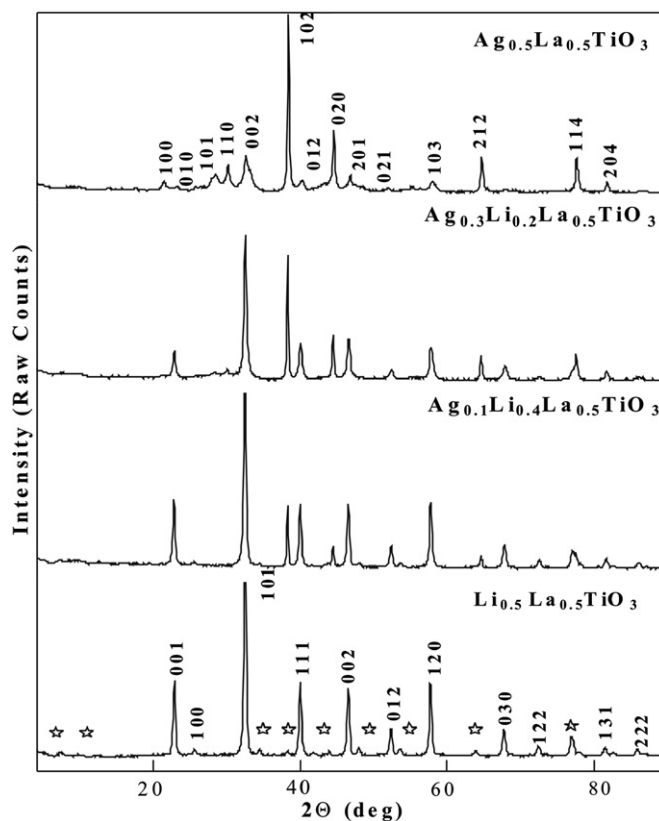


Fig. 1. XRD images of pure and Ag doped lithium lanthanum titanate (LLTO) samples.

sites of tetragonal with twice the interplanar distance in the  $c$ -axis ( $c=2a$ ) resulting in the superlattice diffraction pattern.

It can be observed that the substitution of  $\text{Ag}^+$  introduces a distortion in the unit cell. From the XRD pattern, it is evident that there is a gradual change in the structure with increase in  $\text{Ag}^+$  concentration. The  $\text{Ag}_{0.1}\text{Li}_{0.4}\text{La}_{0.5}\text{TiO}_3$  shows a considerable shift from cubic-superlattice structure to tetragonal. The intensity of the peak corresponding to the plane (101) decreases with  $\text{Ag}^+$  substitution and peak corresponding to the plane (102) starts emerging in  $\text{Ag}_{0.1}\text{Li}_{0.4}\text{La}_{0.5}\text{TiO}_3$  sample which is very specific to tetragonal symmetry.

The  $\text{Ag}_{0.3}\text{Li}_{0.2}\text{La}_{0.5}\text{TiO}_3$  sample shows a mixed phase of cubic and tetragonal structure. The  $\text{Ag}_{0.5}\text{La}_{0.5}\text{TiO}_3$ , which does not contain any lithium ion, forms a complete tetragonal phase which indicates that the regular periodicity in the  $c$ -axis got collapsed while increasing the concentration of  $\text{Ag}^+$  ions and acquires a complete tetragonal structure when  $\text{Ag}^+$  ion replaces all lithium sites. The value of lattice constant for LLTO cubic crystal is  $a=3.887 \text{ \AA}$  which got increased in  $\text{Ag}_{0.5}\text{La}_{0.5}\text{TiO}_3$  as  $a=4.1435 \text{ \AA}$ ,  $c=5.432 \text{ \AA}$  clearly shows the increase in volume of the unit cell due to the larger ionic radius of silver ion compared with the lithium ion.

The average crystallite size calculated for LLTO powder using Debye Scherer formula is 33.69 nm. With  $\text{Ag}^+$  ion substitution the crystallite size increases to 45.5 nm for  $\text{Ag}_{0.3}\text{Li}_{0.2}\text{La}_{0.5}\text{TiO}_3$  sample. The SEM analysis given in Figs. 2(A) and (B) also substantiates the above result. Uniformity of the sample in LLTO is observed through SEM pictures with an average particle size of 80 nm. The SEM image of  $\text{Ag}_{0.3}\text{Li}_{0.2}\text{La}_{0.5}\text{TiO}_3$  shows an increased particle size around 90–120 nm. Due to high temperature calcinations and pre-sintering process, the single crystallite particle tends to join to form the larger aggregates. In this case, particle shows smaller crystallite size than that observed by Electron Microscopy. The Scherer equation estimates the size of one mono-crystal, but if single crystallite particles have sufficient energy to react to form the uniform of two or more crystallites, Scherer's equation fails to estimate the particle size [16]. Therefore the difference between the observed particle size and crystallite

size indicates that each powder particle observed is a combination of two or more cubic perovskite cells than single crystals. The insets in Figs. 2A and B gives a wider area scan to show the uniformity of the sample.

For all the four samples, the photoluminescence (PL) mapping is recorded for excitation wavelength from 200 nm to 600 nm (in steps of 5 nm). The emission observed over the range of 200 nm to 800 nm shows a maximum peak at 470 nm (2.6 eV) corresponding to an excitation maxima of 230 nm (5.38 eV). Fig. 3 shows the emission spectra of LLTO and  $\text{Ag}^+$  doped samples for the same excitation at 230 nm. To the best of our knowledge there is no PL studies carried on LLTO samples in the literature. The PL studies show that the LLTO and  $\text{Ag}^+$  doped LLTO samples excited using a xenon lamp of power 450 W gives an emission at 470 nm which is near the standard blue region. Thus the prepared LLTO sample is a primary colored (blue) nano-ceramic phosphor when excited at a wavelength of 230 nm. With the  $\text{Ag}^+$  substitution, no shift in peak is observed except for the

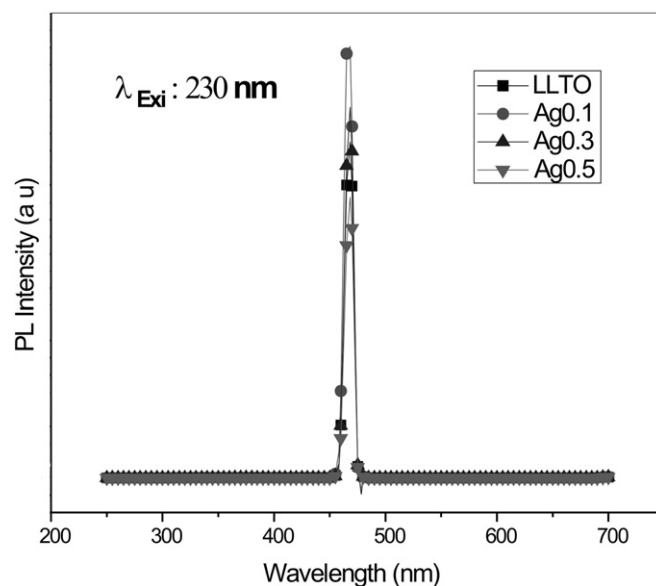


Fig. 3. Emission spectra of pure and Ag doped lithium lanthanum titanate (LLTO) samples.

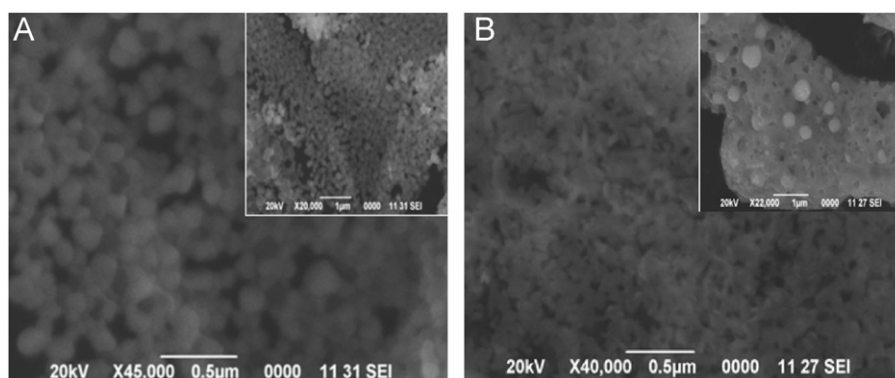


Fig. 2. (A) SEM image for  $\text{Li}_{0.5}\text{La}_{0.5}\text{TiO}_3$ ; (B) SEM image for  $\text{Ag}_{0.3}\text{Li}_{0.2}\text{La}_{0.5}\text{TiO}_3$ .

increase in intensities. The maximum excitation and emission wavelengths correspond to the HOMO and LUMO energy bands. This result indicates that there is no change in electronic states due to the  $\text{Ag}^+$  substitution in LLTO phase.

Fig. 4 shows the cole–cole plots [ $Z'$  (real) Vs  $Z''$  (imaginary) plots] at room temperature (301 K). The equivalent circuits for all the four samples fitted using Z-view software (Figs. 5–8) shows the best fit results with a very low  $\chi^2$  value.

The LLTO powder shows a high frequency semicircle and a low frequency spike. The bulk resistance is found to be very low around  $198.4 \Omega$ . The XRD and SEM result shows that the particle size is in the nano-level which substantiates the present result. The bulk conductivity of LLTO nano-powder is  $1.41 \times 10^{-3} \text{ Scm}^{-1}$  which is one of the highest conductivity reported in the literature [4,5,10,17,18]. The total conductivity of the present sample is  $3.094 \times 10^{-4} \text{ Scm}^{-1}$  at room temperature, which includes the grain boundary and interfacial effects of the LLTO nanoparticles. Most of the literature reports that the grain boundary conductivity of the sample is in the order of  $10^{-5} \text{ Scm}^{-1}$  [5,6,19] which is increased by one order of magnitude in the present nano-LLTO ceramics. This may be due to the availability of proper vacant sites for  $\text{Li}^+$  ion transportation which makes the long range ionic motion possible [20], leading to the higher grain boundary conductivity, even if the size reduction increases the number of grain boundaries.

The  $\text{Ag}^+$  substituted sample Fig. 4(B and C) shows an increase in the grain and grain boundary resistance than the undoped samples. In sample B ( $\text{Ag}_{0.1}\text{Li}_{0.4}\text{La}_{0.5}\text{TiO}_3$ ), the grain conductivity is reduced by one order of magnitude than LLTO nanoparticles. The equivalent circuit

contains high frequency semicircle, constant phase element (CPE) and low frequency Warburg impedance due to the space charge polarization effect [4]. The sample C ( $\text{Ag}_{0.3}\text{Li}_{0.2}\text{La}_{0.5}\text{TiO}_3$ ) shows further reduction in grain

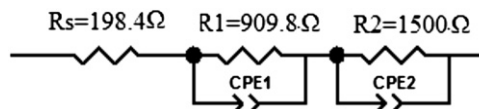


Fig. 5. Equivalent circuits of lithium lanthanum titanate (LLTO).

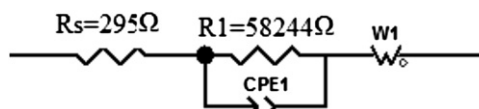


Fig. 6. Equivalent circuits of  $\text{Ag}_{0.1}\text{Li}_{0.4}\text{La}_{0.5}\text{TiO}_3$ .

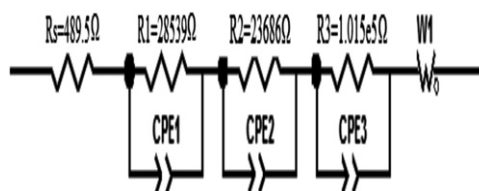


Fig. 7. Equivalent circuits of  $\text{Ag}_{0.3}\text{Li}_{0.2}\text{La}_{0.5}\text{TiO}_3$ .



Fig. 8. Equivalent circuits of  $\text{Ag}_{0.5}\text{La}_{0.5}\text{TiO}_3$ .

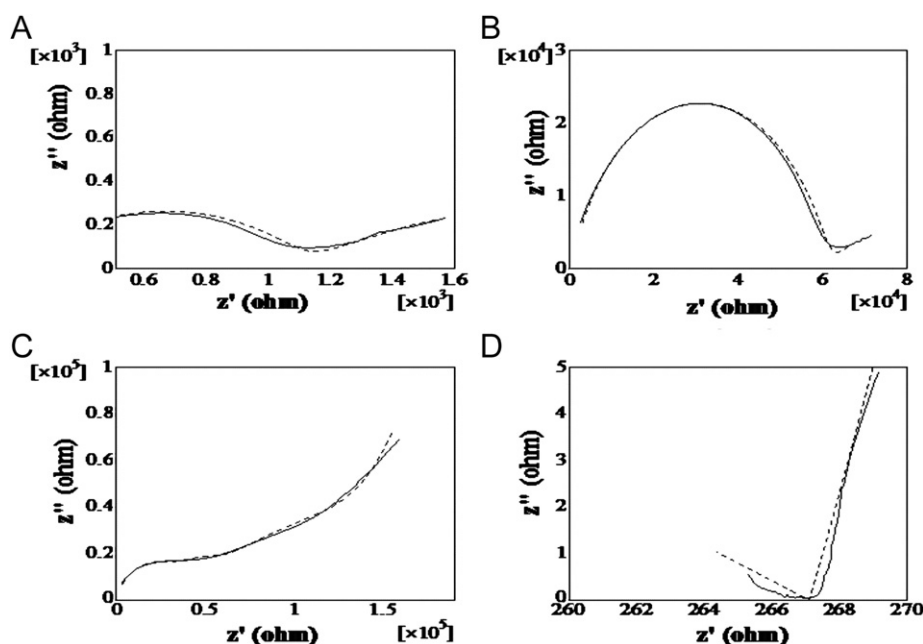


Fig. 4. Cole–Cole plots of pure and Ag doped (LLTO) samples.



Table 1

Grain and grain boundary conductivities of pure and Ag doped lithium lanthanum titanate (LLTO) samples.

Samples	Grain conductivity (S cm <sup>-1</sup> )	Grain boundary conductivity (S cm <sup>-1</sup> )
Li <sub>0.5</sub> La <sub>0.5</sub> TiO <sub>3</sub>	$1.41 \times 10^{-3}$	$1.875 \times 10^{-4}$
Ag <sub>0.1</sub> Li <sub>0.4</sub> La <sub>0.5</sub> TiO <sub>3</sub>	$2.77 \times 10^{-4}$	$1.404 \times 10^{-5}$
Ag <sub>0.3</sub> Li <sub>0.2</sub> La <sub>0.5</sub> TiO <sub>3</sub>	$6.033 \times 10^{-4}$	$2.907 \times 10^{-6}$
Ag <sub>0.5</sub> La <sub>0.5</sub> TiO <sub>3</sub>	$1.166 \times 10^{-3}$	$1.3766 \times 10^{-3}$

conductivity. The complex impedance plot of Ag<sub>0.3</sub>Li<sub>0.2</sub>La<sub>0.5</sub>TiO<sub>3</sub> sample shows three high frequency semicircles. The first semicircle is due to grain resistance; second one due to the grain boundary effect and third semicircle is attributed to the interface in the sample. The total conductivity is reduced to  $5.65 \times 10^{-5}$  S cm<sup>-1</sup> at room temperature. The grain and grain boundary conductivities of the samples were tabulated in Table 1. The result shows that the lithium ions diffuse faster in the grain and grain boundaries of the LLTO nanoparticles than that of the Ag<sup>+</sup> substituted samples. Despite using silver paste as the contact electrode, there is no significant diffusion effect observed in the Ag<sup>+</sup> substituted samples. Hence it is understood that the Ag<sup>+</sup> substitution not only changes the structure but also reduces the available space for the mobility of Li<sup>+</sup> ion. Due to the occupation of the Ag<sup>+</sup> ions in the Li<sup>+</sup> ion sites of the perovskite cage, an impediment is experienced by Li<sup>+</sup> ions in conduction resulting in lower conductivity.

The sample D (Ag<sub>0.5</sub>La<sub>0.5</sub>TiO<sub>3</sub>) shows very high conductivity among all the prepared samples. As there is no lithium ion in the matrix the Ag<sup>+</sup> ions alone contributes to the conductivity and hence both the grain and total conductivity increased from  $10^{-5}$  S cm<sup>-1</sup> to  $10^{-3}$  S cm<sup>-1</sup>. It is to be noted that though Ag<sup>+</sup> ion is bulkier, the conduction obtained is more when the perovskite cage is fully expanded to the occupancy of Ag<sup>+</sup> ion in all the Li<sup>+</sup> sites which becomes a promising candidate. This shows that the Ag<sub>0.5</sub>La<sub>0.5</sub>TiO<sub>3</sub> is a new series of compound in which the Ag<sup>+</sup> ion conduction is in the same order as that of Li<sup>+</sup> ion in LLTO samples.

#### 4. Conclusion

The LLTO nano-powder shows cubic perovskite structure with highly ordered super lattice diffraction pattern. The grain resistance and interface effects were minimized in the nanocrystalline LLTO particles. The Ag<sup>+</sup> substitution disturbs the cubic perovskite (Superlattice) structure of LLTO with the formation of tetragonal phase as the content of Ag<sup>+</sup> increases. As evidenced by the results the transformation end up as all the lithium content of the samples have been replaced by silver ions. The conductivity of Ag<sup>+</sup> partially substituted samples was reduced due to the non-availability of free space for transportation. The Ag<sub>0.5</sub>La<sub>0.5</sub>TiO<sub>3</sub> sample

which did not contain Li<sup>+</sup> shows very high conductivity at room temperature of the order of  $10^{-3}$  S cm<sup>-1</sup>.

#### Acknowledgment

Authors thank University Grant Commission for the necessary financial support through Major Research Project (F.No. 41-842/2012 (SR)). The authors are indebted to Prof. Dr. Austin Suthanthiraraj, University of Madras, Chennai for providing the facilities to carry out the conductivity studies.

#### References

- [1] B. Antoniassi, A.H.M. Gonzalez, S.L. Fernandes, C.F.O. Graeff, Microstructural and electrochemical study of Li<sub>0.5</sub>La<sub>0.5</sub>TiO<sub>3</sub>, Materials Chemistry and Physics 127 (2011) 51–55.
- [2] Odile Bohnke, Quoc Nghi Pham, Anthony Boulant, Joel Emery, Tomas Salkus, Maud Barre, H<sup>+</sup>/Li<sup>+</sup> exchange property of Li<sub>3x</sub>La<sub>2/3-x</sub>TiO<sub>3</sub> in water and in humid atmosphere, Solid State Ionics 188 (2011) 144–147.
- [3] Yuli Xiong, Haizheng Tao, Jiang Zhao, Hao Cheng, Xiujuan Zhao, Effects of annealing temperature on structure and opt-electric properties of ion conducting LLTO thin films prepared by RF magnetron sputtering, Journal of Alloys and Compounds 509 (2011) 1910–1914.
- [4] A.I. Ruiz, M.L. Lopez, M.L. Veiga, C. Pico, Electrical properties of Li<sub>1.33-x</sub>La<sub>3x</sub>Ti<sub>2</sub>O<sub>6</sub> (0.1 < x < 0.3), Solid State Ionics 112 (1998) 291–297.
- [5] C.H. Chen, K. Amine, Ionic conductivity of lithium insertion and extraction of lanthanum lithium titanate, Solid State Ionics 144 (2001) 51–57.
- [6] Ao Mei, Xiao-Liang Wang, Jin-Le Lan, Yu-Chuan Feng, Hong-Xia Geng, Yuan-Hua Lin, Ce-Wen Nan, Role of amorphous boundary layer in enhancing ionic conductivity of lithium lanthanum titanate electrolyte, Electrochimica Acta 55 (2010) 2958–2963.
- [7] D. Mazza, S. Ronchetti, O. Bohnke, H. Duroy, J.L. Fourquet, Modeling Li-ion conductivity in fast ionic conductor Li<sub>2/3-x</sub>La<sub>3x</sub>TiO<sub>3</sub>, Solid State Ionics 149 (2002) 81–88.
- [8] O. Bohnke, C. Bohnke, J. Ould Sid'Ahmed, M.P. Crosnier-Lopez, H. Duroy, F. Le Berre, J.L. Forquet, Lithium ion conductivity in new perovskite oxides [Ag<sub>y</sub>Li<sub>1-y</sub>]<sub>3x</sub>La<sub>2/3-x</sub>1/3-2xTiO<sub>3</sub> (x=0.99 and 0 < y < 1), Chemistry of Materials 13 (2001) 1593–1599.
- [9] Mei-Yu Chen, Ching Yu Chiu, Chia-Ta Chia, J.F. Lee, J.J. Bian, Raman spectra and extended X-ray absorption fine structure characterization of Li<sub>(2-x)/3</sub>Na<sub>x</sub>TiO<sub>3</sub> and Nd<sub>(2-x)/3</sub>Li<sub>x</sub>TiO<sub>3</sub> microwave ceramics, Journal of the European Ceramic Society 30 (2010) 335–339.
- [10] B. Nalini, T. Takeuchi, H. Kageyama, Characterization of europium substituted lithium lanthanum titanate, Solid State Ionics 154–155 (2002) 629–634.
- [11] W.Fergus Jeffrey, Ceramic and polymeric solid electrolytes for lithium ion batteries, Journal of Power Sources 195 (2010) 4554–4569.
- [12] M. Vijayakumar, Y. Inaguma, W. Mashiko, M.P. Crosnier-Lopez, C. Bohnke, Synthesis of fine powders of Li<sub>3x</sub>La<sub>2/3-x</sub>TiO<sub>3</sub> perovskite by polymerizable precursor method, Chemistry of Materials 16 (2004) 2719–2726.
- [13] J. Wolfenstine, J.L. Allen, J. Read, J. Sakamoto, G. Gonzalez-Doncel, Hot-pressed Li<sub>0.33</sub>La<sub>0.57</sub>TiO<sub>3</sub>, Journal of Power Sources 195 (2010) 4124–4128.
- [14] O. Maqueda, F. Saurage, L. Laffond, M.L. Martinez-Sarrion, L. Mestres, E. Bautrin, Structural, microstructural and transport properties study of lanthanum lithium titanate perovskite thin films grown by pulsed laser deposition, Thin Solid Films 516 (2008) 1651–1655.

- [15] Mulki H. Bhat, Anne Miura, Phillipe Vinatier, Alain Levasseur, Kalya J. Rao, Microwave synthesis of lithium lanthanum titanate, *Solid State Communications* 125 (2003) 557–562.
- [16] Emerson R. Camargo, Cristiano M. Barrado, Caue Ribeiro, Elson Longo, Edson R. Leite, Nanosized lead lanthanum titanate (PLT) ceramic powders synthesized by the oxidant peroxo method, *Journal of Alloys and Compounds* 475 (2009) 817–821.
- [17] A.K. Ivanov-Schitz, V.V. Kireev, N.G. Chaban, Growth and investigations of lithium substituted perovskite type ionic conductor, *Solid State Ionics* 136–137 (2000) 501–504.
- [18] Takao Tsurui, Tetsuhiro Katsumata, Yoshiyuki Inaguma, Microstructural analysis of  $\text{La}_{2/3-x}\text{Li}_{3x}\text{TiO}_3$  single crystals and quenched samples observed by high resolution transmission electron microscopy, *Solid State Ionics* 180 (2009) 607–611.
- [19] M.A. Paris, J. Sanz, Li mobility in the orthorhombic  $\text{Li}_{0.18}\text{La}_{0.61}\text{TiO}_3$  perovskite studied by NMR and impedance spectroscopies, *Chemistry of Materials* 12 (2000) 1694–1701.
- [20] H.X. Geng, A. Mei, C. Dong, Y.H. Lin, C.W. Nan, Investigations of structure and electrical properties of  $\text{Li}_{0.5}\text{La}_{0.5}\text{TiO}_3$  ceramics via microwave sintering, *Journal of Alloys and Compounds* 481 (2009) 555–558.